Accurate transition rates for intercombination lines of singly ionized nitrogen

S. S. Tayal*

Department of Physics, Clark Atlanta University, Atlanta, Georgia 30314, USA

(Received 4 October 2010; published 26 January 2011)

The transition energies and rates for the $2s^22p^2\ ^3P_{1,2}$–$2s2p^3\ ^5S^o_2$ and $2s^22p3s$–$2s^22p3p$ intercombination transitions have been calculated using term-dependent nonorthogonal orbitals in the multiconfiguration Hartree-Fock approach. Several sets of spectroscopic and correlation nonorthogonal functions have been chosen to describe adequately term dependence of wave functions and various correlation corrections. Special attention has been focused on the accurate representation of strong interactions between the $2s2p^3\ ^{1,3}P^o_1$ and $2s^22p3s\ ^{1,3}P^o_1$ levels. The relativistic corrections are included through the one-body mass correction, Darwin, and spin-orbit operators and two-body spin-other-orbit and spin-spin operators in the Breit-Pauli Hamiltonian. The importance of core-valence correlation effects has been examined. The accuracy of present transition rates is evaluated by the agreement between the length and velocity formulations combined with the agreement between the calculated and measured transition energies. The present results for transition probabilities, branching fraction, and lifetimes have been compared with previous calculations and experiments.

DOI: 10.1103/PhysRevA.83.012515 PACS number(s): 31.15.ag, 31.15.vj, 32.70.Cs

I. INTRODUCTION

A number of emission features of N II have been observed in the spectra of Titan's upper atmosphere, Saturn's inner magnetosphere, Sun, and other astrophysical objects. Accurate transition probabilities of N II are needed to achieve good fits to high-resolution observations from Cassini, Hubble Space Telescope, and Solar and Heliospheric Observatory. The oscillator strengths and transition probabilities of allowed and intercombination lines in N II are important in the density and temperature diagnostics of astrophysical plasmas. The intercombination transitions occur due to relativistic effects, and are generally sensitive to different correlation effects as well as to high-order Breit interactions. Accurate theoretical calculations of transition rates for intercombination lines are still a challenging problem due to significant canceling contributions for the transition matrix elements and due to sensitivity of results to different correlation corrections.

The prominent N II intercombination lines near 2140 Å correspond to the $2s^22p^2\ ^3P_{1,2}$–$2s2p^3\ ^5S^o_2$ transitions. The intercombination transitions violate the *LS*-coupling selection rule $\Delta S = 0$ and become allowed through the coupling of the $2s2p^3\ ^5S^o_2$ level with the $^3P^o_2$ and $^3D^o_2$ levels. The transition probabilities and branching fraction for the $2s^22p^2\ ^3P_{1,2}$–$2s2p^3\ ^5S^o_2$ transitions and lifetime of the metastable $2s2p^3\ ^5S^o_2$ level have been evaluated in a number of theoretical and experimental studies [1–11]. The calculated and measured branching fraction range from 2.23 to 4.38 and from 2.24 ± 0.06 to 2.45 ± 0.07, respectively. The calculated lifetime varies in the range 3.20–6.45 ms and measured lifetime was determined to be 4.2 ± 0.6 ms in the radio-frequency ion trap experiment [1], 5.4 ± 0.3 ms in the electrostatic ion trap experiment [2], and 5.88 ± 0.03 ms in the heavy-ion storage ring experiment [5]. The latest measured lifetime of the $^5S^o_2$ level from the heavy-ion storage ring deviates from the previous experiments as well as from the latest systematic configuration-interaction (CI) calculation of Brage *et al.* [9]. The heavy-ion storage ring experiment measured lifetime to an unprecedented accuracy of better than 1%, and represents an accuracy improvement by a factor of 10 over the previous experiments. However, the calculation of Brage *et al.* [9] shows excellent agreement with the measured value from the electrostatic ion trap experiment [2]. The branching fraction also shows significant discrepancies between theory and experiment.

The other important N II intercombination transitions that have been studied both theoretically and experimentally correspond to the $2s^22p3s\ ^{3,1}P^o_1$–$2s^22p3p\ ^{3,1}P_J$, $^3S_1$, $^{3,1}D_J$ transitions. The first extensive CI calculation [7] using CIV3 structure code [12] differed from the measured values [4] by about a factor of two. The subsequent CI calculation [8] using CIV3 code focused on the $2p3s$–$2p3p$ transitions and improved upon the previous transition probabilities. A reasonable agreement between theory and experiment was obtained for many transitions, but significant discrepancies remained for some other transitions. It was noted that the accurate determination of energy separations between different levels and of mixing between the $2p3s\ ^3P^o$ and $^1P^o$ levels are important to obtain accurate results for the $2p3s$–$2p3p$ intercombination transitions.

Our attempt in the present work has been to further improve the calculations of transition probabilities for intercombination transitions by improving the flexibility of wave functions to accurately represent the initial and final levels of different transitions to resolve existing discrepancies between theory and experiment. We have also explored the importance of core-valence correlation effects. The aim is to provide definitive calculated oscillator strengths for these and other transitions. We have improved the N II wave functions by using flexible nonorthogonal orbitals to describe term dependence of valence orbitals as well as correlation and relaxation effects. A set of orthogonal orbitals is optimized for each atomic state separately. However, the different sets of orthogonal orbitals thus obtained for different states are not orthogonal to each other. This allowed us to generate a significantly more accurate

*stayal@cau.edu

wave function description of N II levels than those used in previous calculations. Progressively larger calculations have been performed in a systematic manner to make sure that the important correlation corrections are properly accounted for. The strong interactions between the $2s2p^3\ ^{3,1}P^o$ and $2s^22p3s\ ^{3,1}P^o$ states together with the strong spin-orbit mixing between the $2s^22p3s\ ^3P_1^o$ and $^1P_1^o$ levels have been adequately represented. The mass correction, Darwin, spin-orbit, spin-other-orbit, and spin-spin operators of the Breit-Pauli Hamiltonian have been included to represent relativistic effects.

II. COMPUTATIONAL DETAILS

Our calculations are performed using the multiconfiguration Hartree-Fock (MCHF) method [13,14]. In the MCHF approach the atomic state is represented by an atomic state function,

$$\Psi(\alpha LS) = \sum_i c_i \Phi(\alpha_i LS), \tag{1}$$

where the configuration state functions $\Phi(\alpha_i LS)$ are constructed from one-electron functions and α_i defines the coupling of angular momenta of the electrons. The J-dependent atomic state functions are written as a sum over different LS values which couple to give the total angular momentum J,

$$\Psi(\alpha J) = \sum_j a_j \Psi(\alpha_j L_j S_j J). \tag{2}$$

The N II wave functions exhibit large correlation corrections and term dependence of the one-electron orbitals particularly for the $^3D^o$, $^3P^o$, $^1D^o$, and $^1P^o$ terms belonging to the $2s2p^3$, $2s^22p3s$, and $2s^2p3d$ configurations and ^3P and ^1P terms of the $2s^22p^2$ and $2s^22p3p$ configurations. The $2p3p\ ^3S_1$ and $^3P_1$ levels exhibit significant mixing because of closeness of these levels. The low-lying states in N II are defined by $2s^22p^2$, $2s2p^3$, $2s^22pns$, $2s^22pnp$, and $2s^22pnd$ ($n = 3$–4) configurations with two electrons in the $1s^2$ core and remaining four electrons in valence shells. These states show different correlation patterns. We began with the Hartree-Fock calculation for the $1s$, $2p$, and $2p$ orbitals for the $2s^22p^2\ ^3P$ ground state. The $2s$ and $2p$ orbitals in the terms of the $2s^22p^2$, $2s2p^3$, $2s^22p3s$, $2s^22p3p$, and $2s^22p3d$ configurations may be different from each other. The term dependence of $2s$ and $2p$ radial functions is important for the $2s2p^3\ ^3P^o$, $^1P^o$, $^3S^o$, $^1D^o$, $^5S^o$, $2s^22p3s\ ^3P^o$, and $^1P^o$ states. The average radii for the $2s$ and $2p$ orbitals are in the ranges 1.173–1.314 a.u. and 1.100–1.309 a.u., respectively. Similarly, the average radii for the $3s$, $3p$, and $3d$ orbitals vary in the ranges 3.911–3.953 a.u., 4.2701–5.318 a.u., and 4.825–5.274 a.u., while $4p$ and $4d$ orbitals have average radii of 8.904–10.097 a.u. and 9.876–10.329 a.u., respectively. Several sets of nonorthogonal correlation orbitals (l = 0–5) were included in calculation. The correlation orbitals were determined by optimization on the $2s^22p^2\ ^3P$, $2s^22p3s\ ^3P^o$, $2s^22p3s\ ^1P^o$, $2s2p^3\ ^3S^o$, and $2s^22p3p\ ^1P$ states separately. The optimization of spectroscopic and correlation orbitals was carried out in multiconfiguration Hartree-Fock calculations using CI expansions constructed with appropriate orbitals.

The configurations with one-electron and two-electron excitations from the basic configurations to spectroscopic and correlation orbitals were included in the CI expansions. The inclusion of valence-shell correlation is essential to obtain accurate results. We also examined the importance of core-valence correlation by exciting one core $1s$ electron and one valence electron to other spectroscopic and correlation orbitals. The effect of core-valence correlation was found to be very small. The nonorthogonal orbitals provide much greater flexibility to represent term dependence of wave functions than the orthogonal orbitals and also allow one to include correlation effects with a reasonable number of configurations and correlated orbitals [15]. In the construction of CI expansions for fine-structure levels with various J and π we used configurations generated in the previously mentioned excitation scheme for the atomic LS states and with insignificant configurations with coefficients less than 0.00002 omitted from the expansions. These wave functions are then used to calculate excitation energies and the length (f_L) and velocity (f_V) forms of oscillator strengths and transition probabilities for transitions among the fine-structure levels.

III. RESULTS AND DISCUSSION

An important test of the quality of wave functions used in the description of N II levels can be provided by the calculated excitation energies. The excitation energies of fine-structure levels relative to the ground level are given in Table I where our results are compared with measured values from the NIST database (http://physics.nist.gov). We believe that our wave functions correctly represent the main correlation corrections and the interactions between $2s2p^3\ ^{3,1}P^o$ and $2s^22p3s\ ^{3,1}P^o$ states. The composition of the $2s^22p3s\ ^3P_1^o$ level in our calculation is 81.6% $2s^22p3s\ ^3P_1^o$, 1.5% $2s2p^3\ ^3P_1^o$, 3.1% $2p^33s\ ^3P_1^o$, 9.3% $2s^22p3s\ ^1P_1^o$, and 1.0% $2s2p^3\ ^1P_1^o$, while the composition of the $2s^22p3s\ ^1P_1^o$ level is 75.7% $2s^22p3s\ ^1P_1^o$, 8.2% $2s2p^3\ ^1P_1^o$, 2.7% $2p^33s\ ^1P_1^o$, and 9.9% $2s^22p3s\ ^3P_1^o$. The $2s^22p3p\ ^3P$ and ^1P states have relatively higher eigenvector purities with main configurations contributing 94.3% and 94.7%, respectively, for the composition of states. The major correlation correction to these states is provided by the $2p^33p$ configuration with about 3.7% contribution to the composition. A similar situation exists for $2s^22p3p\ ^3D$ and ^3S states. The $2p^4$ configuration makes important correlation contribution to the $2s^22p^2\ ^3P$ ground state as it belongs to the same $n = 2$ complex. The virtual excitations to correlation orbitals make a small important contribution to the $2s2p^3\ ^5S^o$ state with the main configuration contributing 99% to the composition.

The wave functions in our calculations are mostly focused on accurate representation of the $2s^22p^2\ ^3P$ ground state and excited $2s2p^3\ ^5S^o$, $2s^22p3s\ ^3P^o$, $^1P^o$, $2s^22p3p\ ^1P$, ^3D, ^3S, ^1D, and ^1S states. The calculated relative excitation energies for the $2s^22p3s$ and $2s^22p3p$ levels deviate from the experimental values by 66–145 cm^{-1} and 38–282 cm^{-1}, respectively. The calculated excitation energy for the $2s2p^3\ ^5S^o$ state is lower than the experiment by 243 cm^{-1}. The levels of the $2s^22p3d$ configuration are also generally very well represented. The calculated energies of the levels of $2s^22p3d\ ^1D^o$, $^3D^o$, and $^3P^o$ states deviate from the experiment by less

TABLE I. Comparison of calculated and experimental energy levels (cm^{-1}). Lifetimes (s) of excited levels are also listed. Numbers in square brackets denote powers of 10.

Index	Term	J	Experiment	Calculation	τ(Present)	τ(FT[a])
1	$2s^22p^2\ ^3P$	0	0	0.0		
2	$2s^22p^2\ ^3P$	1	48.7	40.6		
3	$2s^22p^2\ ^3P$	2	130.8	121.8		
4	$2s^22p^2\ ^1D$	2	15316.2	15758.3		
5	$2s^22p^2\ ^1S$	0	32688.8	33214.2		
6	$2s2p^3\ ^5S$	2	46784.6	46541.5	6.14[−3]	5.62[−3]
7	$2s2p^3\ ^3D$	3	92237.2	92636.9	2.62[−9]	2.69[−9]
8	$2s2p^3\ ^3D$	2	92250.3	92646.8	2.61[−9]	2.68[−9]
9	$2s2p^3\ ^3D$	1	92251.8	92654.5	2.61[−9]	2.67[−9]
10	$2s2p^3\ ^3P$	2	109217.6	109979.8	7.53[−10]	7.88[−10]
11	$2s2p^3\ ^3P$	1	109216.6	109981.9	7.52[−10]	7.87[−10]
12	$2s2p^3\ ^3P$	0	109223.5	109983.1	7.51[−10]	7.86[−10]
13	$2s2p^3\ ^1D$	2	144187.9	145642.2	3.11[−10]	3.18[−10]
14	$2s^22p3s\ ^3P$	0	148908.6	149053.9	9.24[−10]	8.82[−10]
15	$2s^22p3s\ ^3P$	1	148940.2	149081.4	8.72[−10]	7.07[−10]
16	$2s^22p3s\ ^3P$	2	149076.5	149210.9	9.22[−10]	8.80[−10]
17	$2s^22p3s\ ^1P$	1	149187.8	149253.7	2.58[−10]	2.62[−10]
18	$2s2p^3\ ^3S$	1	155126.7	156112.2	8.96[−11]	9.35[−11]
19	$2s^22p3p\ ^1P$	1	164610.8	164648.7	2.74[−8]	3.08[−8]
20	$2s^22p3p\ ^3D$	1	166521.7	166585.6	1.18[−8]	1.27[−8]
21	$2s^22p3p\ ^3D$	2	166582.5	166643.7	1.18[−8]	1.27[−8]
22	$2s^22p3p\ ^3D$	3	166678.6	166734.8	1.18[−8]	1.27[−8]
23	$2s2p^3\ ^1P$	1	166765.7	168685.9	2.03[−10]	2.22[−10]
24	$2s^22p3p\ ^3S$	1	168892.2	169023.9	6.66[−9]	6.87[−9]
25	$2s^22p3p\ ^3P$	0	170572.6	170667.8	5.81[−9]	6.14[−9]
26	$2s^22p3p\ ^3P$	1	170607.9	170700.7	5.81[−9]	6.14[−9]
27	$2s^22p3p\ ^3P$	2	170666.2	170756.7	5.80[−9]	6.13[−9]
28	$2s^22p3p\ ^1D$	2	174212.0	174432.9	6.89[−9]	7.34[−9]
29	$2s^22p3p\ ^1S$	0	178273.4	178555.7	4.65[−9]	4.73[−9]
30	$2s^22p3d\ ^3F$	2	186511.6	186918.8	4.16[−9]	6.82[−9]
31	$2s^22p3d\ ^3F$	3	186571.0	186981.3	6.39[−9]	7.59[−9]
32	$2s^22p3d\ ^3F$	4	186652.5	187060.3	8.39[−9]	8.76[−9]
33	$2s^22p3d\ ^1D$	2	187091.4	187184.3	3.49[−10]	3.47[−10]
34	$2s^22p3d\ ^3D$	1	187437.6	187499.3	2.34[−10]	2.30[−10]
35	$2s^22p3d\ ^3D$	2	187461.9	187523.4	2.36[−10]	2.31[−10]
36	$2s^22p3d\ ^3D$	3	187491.9	187553.1	2.36[−10]	2.31[−10]
37	$2s^22p3d\ ^3P$	2	188857.4	188928.1	3.91[−10]	3.91[−10]
38	$2s^22p3d\ ^3P$	1	188909.2	188977.4	3.91[−10]	3.91[−10]
39	$2s^22p3d\ ^3P$	0	188937.2	189009.3	3.91[−10]	3.91[−10]
40	$2s^22p3d\ ^1F$	3	189335.2	189797.2	2.73[−10]	2.57[10]
41	$2s^22p3d\ ^1P$	1	190120.2	190259.2	3.99[−10]	3.72[−10]

[a]Reference [10].

than 100 cm^{-1}. The overall agreement between theory and experiment for the levels of $2s2p^3$ configuration is satisfactory, with average deviation of about 800 cm^{-1}. The present description of N II states represents an improvement over the previous calculations. In the calculations of Vaeck *et al.* [8] and Froese Fischer and Tachiev [10] the diagonal elements of the *LS* Hamiltonian matrices were adjusted to bring the calculated energies close to the observation, whereas our calculations are completely *ab initio*. We also present lifetimes of excited levels in Table I where the present MCHF results have been compared with the MCHF results of Froese Fischer and Tachiev [10]. We calculated transition probabilities of all possible $E1$ transitions between the states considered in our work for the calculation of lifetimes. The present lifetimes are generally within 10% of the earlier calculation for most of the levels.

A. Transition rates for the $2s^22p^2\ ^3P_{1,2}$–$2s2p^3\ ^5S^o_2$ intercombination lines

In Table II, we present transition energies and rates for the $2s^22p^2\ ^3P_J$–$2s2p^3\ ^5S^o_2$ intercombination $E1$ and magnetic quadrupole $M2$ lines. The present transition rates have been compared with the previous calculations of Froese Fischer and Tachiev [10] and Brage *et al.* [9]. The agreement between calculated and measured transition energies is about 0.5%. We believe that our wave functions correctly represent main

TABLE II. Transition energies (in cm^{-1}) and rates (in s^{-1}) for the $2s^22p^2\ ^3P_J$–$2s2p^3\ ^5S^o_2$ intercombination ($E1$) and magnetic quadrupole ($M2$) lines in N II. The branching ratio for the $2s^22p^2\ ^3P_J$–$2s2p^3\ ^5S^o_2$ transitions and lifetime (ms) for the $^5S^o_2$ level are also given. Numbers in square brackets denote powers of 10.

Transition		Δ(Expt.)	Δ(Theor.)	Present	FT[a]	BHL[b]	Experiment
Transition rates							
$2s^22p^2\ ^3P_1$–$2s2p^3\ ^5S^o_2$	$E1$	46735.9	46501.0	47.01	51.55	53.6	
$2s^22p^2\ ^3P_2$–$2s2p^3\ ^5S^o_2$	$E1$	46653.8	46420.4	115.76	126.60	130.6	
$2s^22p^2\ ^3P_0$–$2s2p^3\ ^5S^o_2$	$M2$	46784.6	46541.5	9.85[−4]	9.57[−4]		
$2s^22p^2\ ^3P_1$–$2s2p^3\ ^5S^o_2$	$M2$	46735.9	46501.0	2.11[−3]	2.14[−3]		
$2s^22p^2\ ^3P_2$–$2s2p^3\ ^5S^o_2$	$M2$	46653.8	46420.4	1.62[−3]	1.65[−3]		
Branching ratio				2.46	2.46	2.44	2.45 ± 0.07[c]
							2.27 ± 0.23[d]
							2.24 ± 0.06[e]
Lifetime				6.143	5.615	5.43	5.4 ± 0.3[f]
							5.88 ± 0.03[g]
							4.2 ± 0.6[h]

[a]Reference [10].
[b]Reference [9].
[c]Reference [3].
[d]Reference [6].
[e]Reference [4].
[f]Reference [2].
[g]Reference [5].
[h]Reference [1].

correlation corrections and relaxation effects. The errors in theoretical transition rates can be due to inaccuracies in the *ab initio* calculations of transition energies and of the matrix elements of the transition operator. The $E1$ transitions rates scale as third power of the transition energy and $M2$ transition rates scale with the fifth power of transition energy. The uncertainty in the calculated transition rates due to the inaccuracies in transition energies has been minimized by the semiempirical adjustment to the experimental transition energies. The previous calculations adjusted diagonal energies of LS blocks to reproduce experimental energies. The present transition rates for $E1$ transitions are lower from the previous calculations of Brage *et al.* [9] and Froese Fischer and Tachiev [10] by about 12% and 9%, respectively. There is excellent agreement between the present and previous MCHF calculation for the $M2$ transitions. Our calculated branching ratio shows excellent agreement with the previous calculations and with the experimental results of Bridges *et al.* [3], as also quoted in the paper of Brage *et al.* [9], and Curry *et al.* [6]. The measured branching ratio of Musielok *et al.* [4] is lower than the theoretical results by about 8%. The experimental results are also available for the lifetime of the $^5S^o_2$ level that can be compared with theoretical results. The most recent experimental result using a heavy-ion storage ring [5] represents significant improvement in accuracy over the previous radio-frequency and electrostatic ion trap experiments [1,2], and are somewhat larger than the previous experiments. The present lifetime differs from the latest heavy-ion storage experiment by about 4% and from the previous calculations of Brage *et al.* [9] and Froese Fischer and Tachiev [10] by 13% and 9%, respectively. It may be noted that the calculation of Brage *et al.* [9] shows excellent agreement with the electrostatic ion trap experiment [2]. However, the present calculation and the calculation of Froese Fischer and Tachiev [10] are in better agreement with the latest and more accurate heavy-ion storage experiment [5] than the calculation of Brage *et al.* [9]. The lifetime from two MCHF calculations are within 5% of the heavy-ion storage measurement. We have also examined the importance of core-valence correlation effects for the transition rates, and found these to be insignificant. The spin-spin interaction is important to obtain accurate transition rates. It is clear from Table II that the $M2$ transition rates make insignificant contributions to the lifetime of the $2s2p^3\ ^5S^o_2$ level. The present calculated transition rates should be accurate to about 5%.

B. Transition rates for the $2s^22p3s$–$2s^22p3p$ intercombination lines

The oscillator strengths and transition probabilities for $2s^22p3s$–$2s^22p3p$ intercombination transitions are listed in Table III, where our results are compared with other calculations and experiment. There is generally a good agreement between the present length and velocity values. The length results are shown in the first row and the velocity values are given in the second row for each transition. The calculated values of Bell *et al.* [7] show discrepancies of a factor of two with the measured values, and these calculations were improved by Vaeck *et al.* [8]. In Table III we have shown the comparison of our results with the calculation of Vaeck *et al.* [8] only. The oscillator strengths and transition probabilities from the work of Froese Fischer and Tachiev [10] are also shown. Our calculation represents significant improvement over the previous calculations for many transitions. Most of our effort in the present work has been to improve the representation of different states of the $2s^22p3s$ and $2s^22p3p$ configurations. Our transition energies are in excellent

TABLE III. Oscillator strengths and transition probabilities for the $2s^2 2p 3s$–$2s^2 2p 3p$ intercombination transitions. Numbers in square brackets denote powers of 10.

	Present work		VFB[a]		FT[b]		
Transition	f_{ik}	A_{ki}	f_{ik}	A_{ki}	f_{ik}	A_{ki}	Experiment[c]
$3s^1P_1^o$–$3p^3P_0$	0.0116	1.060[7]	0.0094	8.642[6]	0.0093	8.534[6]	1.16 ± 0.10[7]
	0.0096	8.870[6]	0.0092	8.440[6]			
$3s^3P_1^o$–$3p^1S_0$	0.0129	2.214[7]	0.0108	1.853[7]	0.0111	1.909[7]	2.36 ± 0.33[7]
	0.0130	2.183[7]	0.0106	1.830[7]			
$3s^3P_1^o$–$3p^1P_1$	0.0272	4.450[6]	0.0212	3.475[6]	0.0215	3.517[6]	6.11 ± 0.7[6]
	0.0254	4.159[6]	0.0194	3.169[6]			
$3s^1P_1^o$–$3p^3D_1$	0.0132	2.621[6]	0.0128	2.534[6]	0.0119	2.386[6]	2.29 ± 0.21[6]
	0.0136	2.736[6]	0.0112	2.239[6]			
$3s^1P_1^o$–$3p^3S_1$	0.0106	2.756[6]	0.0089	2.291[6]	0.0094	2.434[6]	2.67 ± 0.21[6]
	0.0100	2.585[6]	0.0081	2.090[6]			
$3s^1P_1^o$–$3p^3P_1$	0.0093	2.837[6]	0.0076	2.329[6]	0.0075	2.305[6]	3.48 ± 0.32[6]
	0.0079	2.419[6]	0.0075	2.282[6]			
$3s^1P_1^o$–$3p^3D_2$	0.0300	3.585[6]	0.0290	3.472[6]	0.0270	3.273[6]	3.32 ± 0.32[6]
	0.0307	3.746[6]	0.0256	3.099[6]			
$3s^1P_1^o$–$3p^3P_2$	0.0130	2.399[6]	0.0106	1.954[6]	0.0104	1.919[6]	2.72 ± 0.25[6]
	0.0106	1.981[6]	0.0102	1.873[6]			
$3s^3P_1^o$–$3p^1D_2$	0.0588	1.504[7]	0.0465	1.188[7]	0.0472	1.205[7]	1.33 ± 0.11[7]
	0.0588	1.499[7]	0.0546	1.395[7]			

[a]Reference [8].
[b]Reference [10].
[c]Reference [4].

agreement with experiment and deviate by 100 cm^{-1} or less. We used experimental transition energies to minimize the inaccuracies in transition rates.

The length values remain stable with respect to the addition of more configurations and are preferred over the velocity values. Our results are larger than the other two calculations for all transitions in Table III. The present length transition rates show excellent agreement with experiment and are within the measured uncertainties for the $2s^2 2p 3s\ ^1P_1^o$–$2s^2 2p 3p\ ^3P_0$, $^3S_1$, $^3P_1$, $^3D_2$, and $2s^2 2p 3s\ ^3P_1^o$–$2s^2 2p 3p\ ^1S_0$ intercombination transitions. There is improved agreement between theory and experiment for the $2s^2 2p 3s\ ^1P_1^o$–$2s^2 2p 3p\ ^3P_2$ and $^1D_2$ transitions. The present transition rate for the $2s^2 2p 3s\ ^3P_1^o$–$2s^2 2p 3p\ ^1P_1$ transition is larger than the previous calculations by about 27%, but still lower by 27% than experiment. The previous theoretical calculations show better agreement with experiment for the $2s^2 2p 3s\ ^3P_1^o$–$2s^2 2p 3p\ ^3D_1$ transition where our result differs slightly from the experimental upper limit. The length and velocity values of oscillator strengths for the other $2s^2 2p 3s$ and $2s^2 2p 3p$ transitions are in given Table IV, and our results are compared with the previous extensive calculations of Vaeck *et al.* [8] and Froese Fischer and Tachiev [10]. An excellent agreement between three independent calculations can be noted. The oscillator strengths for the $2s^2 2p 3s$–$2s^2 2p 3p$ intercombination transitions have significant strengths, but are smaller by a factor or so than the $2s^2 2p 3s$–$2s^2 2p 3p$ dipole-allowed transitions.

For the sake of completeness, we have also compared present oscillator strengths for $E1$ dipole-allowed transitions from the $2s^2 2p^2\ ^3P_{0,1,2}$ levels to all odd parity levels of the $2s 2p^3$, $2s^2 2p 3s$, $2s^2 2p 3d$, and $2s^2 2p 4s$ configurations in Fig. 1. Our results are compared with previously available calculations of Bell *et al.* [7] and Froese Fischer and Tachiev [10]. There is excellent agreement with previous calculations. All three independent calculations are within 5% of each other. The agreement between different calculations suggests that the oscillator strengths for these transitions are very well established to an accuracy of about 5%.

TABLE IV. Oscillator strengths for the $2s^2 2p 3s$–$2s^2 2p 3p$ dipole-allowed transitions.

	Present work		VFB[a]		FT[b]
Transition	f_L	f_V	f_L	f_V	f_{ik}
$3s^3P_1^o$–$3p^3P_0$	0.1024	0.0854	0.1011	0.0987	0.0965
$3s^1P_1^o$–$3p^1S_0$	0.1124	0.1105	0.1136	0.1124	0.1130
$3s^1P_1^o$–$3p^1P_1$	0.1834	0.1721	0.1693	0.1538	0.1628
$3s^3P_0^o$–$3p^3D_1$	0.4198	0.4011	0.4144	0.3935	0.4053
$3s^3P_1^o$–$3p^3D_1$	0.0880	0.0870	0.0890	0.0859	0.0864
$3s^3P_2^o$–$3p^3D_1$	0.0039	0.0037	0.0038	0.0037	0.0037
$3s^3P_0^o$–$3p^3S_1$	0.0934	0.0875	0.0918	0.0837	0.0938
$3s^3P_1^o$–$3p^3S_1$	0.0775	0.0728	0.0778	0.0708	0.0791
$3s^3P_2^o$–$3p^3S_1$	0.0770	0.0730	0.0759	0.0688	0.0772
$3s^3P_0^o$–$3p^3P_1$	0.3249	0.2700	0.3154	0.3082	0.3007
$3s^3P_1^o$–$3p^3P_1$	0.0721	0.0668	0.0714	0.0698	0.0677
$3s^3P_2^o$–$3p^3P_1$	0.0911	0.0764	0.2842	0.2740	0.2770
$3s^3P_1^o$–$3p^3D_2$	0.2828	0.2701	0.2842	0.2740	0.2770
$3s^3P_2^o$–$3p^3D_2$	0.0595	0.0571	0.0588	0.0567	0.0574
$3s^3P_1^o$–$3p^3P_2$	0.1252	0.1063	0.1235	0.1207	0.1177
$3s^3P_2^o$–$3p^3P_2$	0.2586	0.2160	0.2511	0.2453	0.2407
$3s^3P_1^o$–$3p^1D_2$	0.5179	0.5168	0.4954	0.5790	0.4853
$3s^3P_2^o$–$3p^3D_3$	0.3480	0.3327			0.3359

[a]Reference [8].
[b]Reference [10].

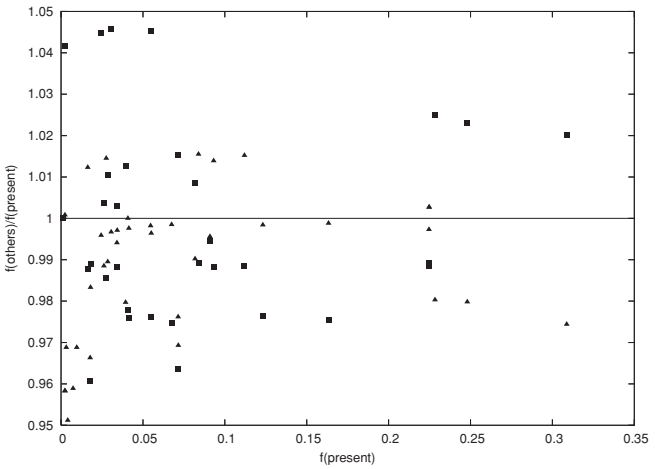

FIG. 1. Comparison of present oscillator strengths for the dipole-allowed transitions with other theoretical calculations. (Solid triangles) Calculation of Bell *et al.* [7]. (Solid rectangles) Calculation of Froese Fischer and Tachiev [10].

IV. CONCLUSION

In conclusion, we have presented fairly extensive calculations of oscillator strengths and transition probabilities for allowed and intercombination transitions. Our large-scale CI calculations have been performed in a systematic approach to include all important valence-shell and core-valence correlation effects. We have made extensive use of nonorthogonal orbital sets for the representation of term dependence of one-electron orbitals in different atomic states. A good agreement with the latest measured value from the heavy-ion storage experiment and the calculated result of Froese Fischer and Tachiev [10] has been obtained for the lifetime of the $2s2p^3\ {}^5S^o_2$ level. The calculated branching ratio $A(2s^22p^2\ {}^3P_2–2s2p^3\ {}^5S^o_2)/A(2s^22p^2\ {}^3P_1–2s2p^3\ {}^5S^o_2)$ is in excellent agreement with measured values and other calculations. Our results for the intercombination $2s^22p3s–2s^22p3p$ transitions normally agree very well with experiment except for the $2s^22p3s\ {}^3P^o_1–2s^22p3p\ {}^1P_1$ transition. The discrepancies with experiment for the intercombination $2s^22p3s\ {}^3P^o_1–2s^22p3p\ {}^1P_1$ transition is about 27%. The oscillator strengths and transition probabilities for weak intercombination transitions are very sensitive to electron correlation corrections in singlet and triplet states of both odd and even parities and, therefore, to the choice of wave functions. Our calculations are more extensive and thorough compared to existing other theoretical work, and show an overall better agreement with the experimental results. The present calculated results for the dipole-allowed transitions are in excellent agreement with previous extensive and reliable calculations.

The overall uncertainty in the present calculated transition rates for the $2s^22p^2\ {}^3P_{1,2}–2s2p^3\ {}^5S^o_2$ and $2s^22p3s–2s^22p3p$ intercombination transitions is estimated to be about 5% for most transitions and at worst no more than 10% for a few transitions. The estimate is based on the agreement between the present calculated and measured transition energies (0.5% or better) as well as the comparison of present calculated transition rates, branching ratio, and lifetimes with the latest and reliable experiments. For example, calculated branching ratio is in excellent agreement with experiments and the lifetime for the $^5S^o_2$ level is within 5% of the measured value from the heavy-ion storage ring experiment with quoted accuracy of better than 1%. Our transition rates for the $2s^22p3s–2s^22p3p$ intercombination transitions are within the experimental uncertainty for most transitions.

ACKNOWLEDGMENTS

This work was supported by National Aeronautics and Space Administration under Grant No. NNX09AB63G from the Planetary Atmospheres Program.

[1] R. D. Knight, Phys. Rev. Lett. **48**, 792 (1982).
[2] A. G. Calamai and C. E. Johnson, Phys. Rev. A **44**, 218 (1991).
[3] J. M. Bridges, W. L. Wiese, and Griesmann, in *Goddard High Resolution Spectrograph Science Symposium, Greenbelt, Maryland*, No. 40 (Goddard Space Flight Center, Greenbelt, 1996).
[4] J. Musielok, J. M. Bridges, S. Djurovic, and W. L. Wiese, Phys. Rev. A **53**, 3122 (1996).
[5] E. Träbert, A. Wolf, E. H. Pinnington, J. Linkemann, E. J. Knystautas, A. Curtis, N. Bhattacharya, and H. G. Berry, Phys. Rev. A **58**, 4449 (1998).
[6] J. J. Curry, N. D. Gibson, and J. E. Lawler, Astron. Astrophys. **321**, 1021 (1997).
[7] K. L. Bell, A. Hibbert, and R. P. Stafford, Phys. Scr. **52**, 240 (1995).
[8] N. Vaeck, J. Fleming, K. L. Bell, A. Hibbert, and M. R. Godefroid, Phys. Scr. **56**, 603 (1997).
[9] T. Brage, A. Hibbert, and D. S. Leckrone, Astrophys. J. **478**, 423 (1997).
[10] C. Froese Fischer and G. Tachiev, At. Data Nucl. Data Tables **87**, 1 (2004).
[11] D. G. Ellis, Phys. Rev. A **47**, 161 (1993).
[12] A. Hibbert, Comput. Phys. Commun. **9**, 141 (1975).
[13] C. Froese Fischer, Comput. Phys. Commun. **176**, 559 (2007).
[14] O. Zatsarinny and C. Froese Fischer, Comput. Phys. Commun. **124**, 247 (1999).
[15] O. Zatsarinny and S. S. Tayal, J. Phys. B **34**, 1299 (2001).